NJC

PAPER

View Article Online
View Journal | View Issue

Cite this: *New J. Chem.*, 2017, **41**, 14431

Array-based detection of isomeric and analogous analytes employing synthetically modified fluorophore attached β-cyclodextrin derivatives†

Sauradip Chaudhuri, Dana J. DiScenza, Benjamin Smith, Reid Yocum and Mindy Levine *

Received 10th August 2017,
Accepted 23rd October 2017

DOI: 10.1039/c7nj02968c

rsc.li/njc

Reported herein is a sensitive and selective array-based sensing strategy based on differential interactions with three supramolecular cyclodextrin–fluorophore sensors. Each interaction results in a distinct fluorescence modulation response, and linear discriminant analyses of these responses results in 100% successful classification of three classes of isomeric analytes and two classes of analogous analytes. Calculated limits of detection for this system are at or near literature-reported levels of concern.

Introduction

The selective detection and accurate quantification of structurally similar analytes is a major challenge for scientists, as structurally similar analytes often have widely disparate toxicities.[1] The most common strategy is to use mass spectrometry methods, such as liquid chromatography-mass spectrometry (LC-MS)[2] or gas chromatography-mass spectrometry (GC-MS).[3] However, there are significant drawbacks associated with this approach, including the costs and time necessary to conduct such analyses,[4] which limits the ability to conduct high throughput assays.[5]

An alternate strategy is to use array-based sensing systems, which have recently gained in popularity.[6] This approach relies on the development of a chemical signature for each analyte based on analyte-specific interactions with a sensor series. Array-based sensing systems can be combined with supramolecular sensors, which rely on differential non-covalent interactions of analytes with supramolecular hosts, including cyclodextrins,[7] fluorescent polymers,[8] molecularly imprinted polymers,[9] and metal–organic frameworks (MOFs).[10]

Although supramolecular array-based systems overcome many challenges associated with mass-spectrometry based detection methods, the analyte scope explored in most of these reports have been limited to aromatic small molecules.[11] In a real-world contaminated environment, the nature of the various pollutants is highly complex,[12] and includes mixtures of aromatic and non-aromatic compounds.[13] This kind of situation requires the development of a sensing system which is rapid, simple, and efficient in classifying a broad range of persistent organic pollutants (POPs).[14]

Our group has previously reported the use of β-cyclodextrin and γ-cyclodextrin in array-based detection systems for the sensing of a wide variety of environmental toxicants and POPs.[15] The sensing strategy is based on cyclodextrin promoted analyte-to-fluorophore energy transfer as well as cyclodextrin-promoted, analyte-induced fluorescence modulation. In the fluorescence modulation systems, the fluorophore was added to the cyclodextrin solution prior to analyte addition, which can result in fluorophore–cyclodextrin binding that reduces the cyclodextrin's ability to bind the target analyte. As such, introduction of the analyte to the fluorophore–cyclodextrin solution requires the analyte–cyclodextrin association constants to be higher than those of the fluorophore–cyclodextrin (Fig. 1A), or it requires the formation of higher order association complexes between the

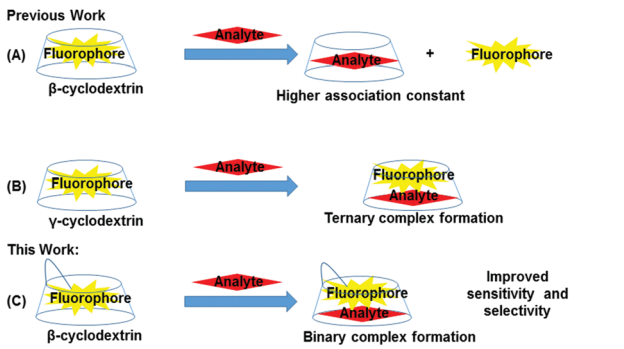

Fig. 1 Schematic illustration of this work compared to previously published work.

Department of Chemistry, University of Rhode Island, 140 Flagg Road, Kingston, RI 02881, USA. E-mail: mlevine@chm.uri.edu, mindy.levine@gmail.com; Fax: +1-401-874-5072; Tel: +1-401-874-4243

† Electronic supplementary information (ESI) available: Detailed synthetic procedures; detailed procedures for fluorescence modulation, limit of detection, and array analysis experiments; summary figures and tables of all data; copies of NMR spectra of all new compounds. See DOI: 10.1039/c7nj02968c

analyte, cyclodextrin and fluorophore (Fig. 1B). Such higher order association complexation is probable only for γ-cyclodextrin.[16]

Herein, we report the development of an array-based detection system using fluorophore-functionalized perbenzylated β-cyclodextrin sensors, which enables binary complex formation between the functionalized cyclodextrin and the target analyte (Fig. 1C). Each sensor is selective, meaning the array is able to distinguish three classes of isomeric analytes and two classes of structurally similar analytes, with 100% classification accuracy. High sensitivity is demonstrated as well, with limits of detection approaching or surpassing literature-reported levels of concern. Finally, preliminary efforts at using this system for the accurate identification of binary analyte mixtures are also reported.

Experimental section

Materials and methods

All the reagents were obtained from Sigma Aldrich or Fisher Scientific and used without further purification, unless otherwise noted. β-Cyclodextrin was dried in the oven prior to use. Reagent grade solvents (99.9% purity) were used for the synthetic reactions.

Fluorescence modulation experiments

Fluorescence emission spectra were obtained using a Shimadzu RF-5301PC spectrophotofluorimeter with 3 nm excitation and 3 nm emission slit widths. 0.5 mL of **S1**, **S2**, or **S3** solutions (5 μM in DMSO) and 2 mL of deionized water were combined in a quartz cuvette. The solution was excited at 320 nm, and the fluorescence emission spectra were recorded.

The fluorescence emission spectra were integrated *vs.* wavenumber on the *X*-axis, and the fluorescence modulation was measured as the ratio of the integrated emission of the fluorophore in the presence of the analyte to integrated emission of the fluorophore in the absence of the analyte (eqn (1)):

$$\text{Fluorescence modulation} = \text{Fl}_{\text{analyte}}/\text{Fl}_{\text{blank}} \qquad (1)$$

where $\text{Fl}_{\text{analyte}}$ is the integrated fluorescence emission of the fluorophore in the presence of 10 μL of analyte (1 mg mL^{-1} in THF), and Fl_{blank} is the integrated fluorescence emission of the fluorophore in the absence of the analyte.

Array generation experiments

Array analysis was performed using SYSTAT 13 statistical computing software with the following settings:

(a) Classical discriminant analysis
(b) Grouping variable: analytes
(c) Predictors: **S1**, **S2**, and **S3**
(d) Long-range statistics: mahal

Limit of detection experiments

The limit of detection (LOD) is defined as the lowest concentration of analyte at which a signal can be detected. To determine this value, the following steps were performed for each cyclodextrin-analyte combination. In a quartz cuvette, 0.5 mL of **S1**, **S2**, or **S3** solutions (5 μM in DMSO) and 2 mL of deionized water were combined. The solution was excited at 320 nm, and the fluorescence emission spectra were recorded starting at 330 nm. Six repeat measurements were taken.

Next, 2 μL of analyte (1 mg mL^{-1} in THF) was added, and again the solution was excited at the fluorophore's excitation wavelength, and the fluorescence emission spectra were recorded. Six repeat measurements were taken. This step was repeated for 4 μL of analyte, 6 μL of analyte, 8 μL of analyte, 10 μL of analyte, 12 μL of analyte, 14 μL of analyte, 16 μL of analyte, 18 μL of analyte, and 20 μL of analyte.

All of the fluorescence emission spectra were integrated *vs.* wavenumber on the *X*-axis, and calibration curves were generated. The curves plotted the analyte concentration in μM on the *X*-axis, and the fluorescence modulation ratio on the *Y*-axis. The curve was fitted to a straight line and the equation of the line was determined.

The limit of detection is defined according to eqn (2):

$$\text{LOD} = 3(\text{SD}_{\text{blank}})/m \qquad (2)$$

where SD_{blank} is the standard deviation of the blank sample and m is the slope of the calibration curve.

Results and discussion

We employed a series of three cyclodextrin-based supramolecular sensors (Fig. 2) for the detection of a broad variety of small molecule analytes (Fig. 3). In these sensors, the perbenzylated β-cyclodextrin cavity acts as the receptor domain, and the attached fluorophore units act as the transducers, which are responsible for fluorescence-based responses to changes in their environment in the presence of the target analyte. The covalent attachment strategy used in sensors **S2** and **S3**, with one and two degrees of functionalization on the primary rim, respectively, ensures the close proximity of the fluorophore

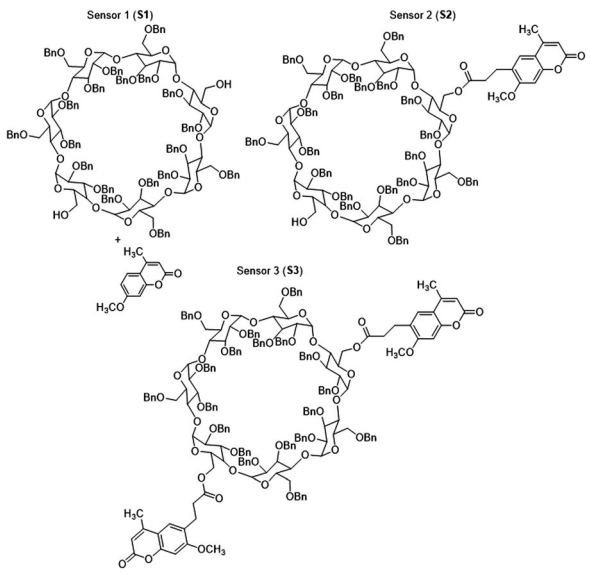

Fig. 2 Structures of sensors **S1–S3**.

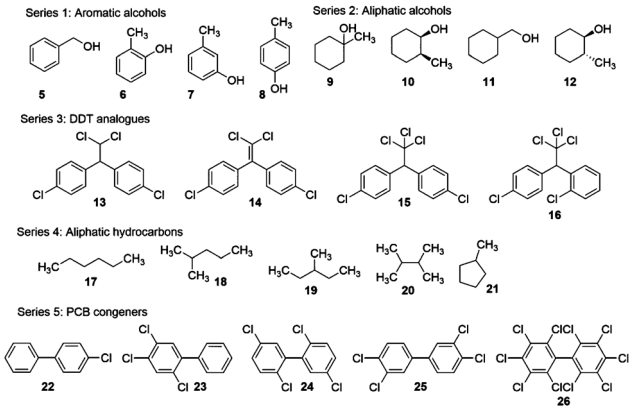

Fig. 3 Structures of small molecule analytes **5–26**.

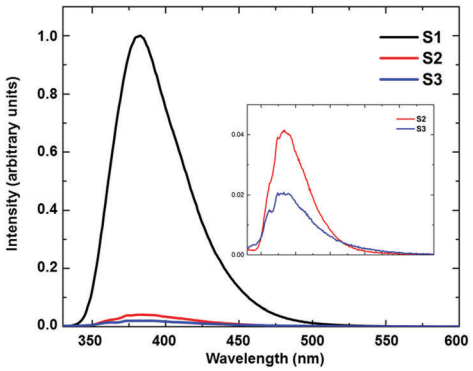

Fig. 4 Fluorescence emission spectra of supramolecular hosts **S1–S3** (1 μM) (inset shows the fluorescence of **S2** and **S3** in more detail) in 80 : 20 water–DMSO solution. (λ_{ex} = 320 nm; 3 nm excitation slit width; 3 nm emission slit width).

units to the cyclodextrin receptor cavity, thereby facilitating productive fluorophore–analyte interactions. In contrast, sensor **S1** is a non-covalent combination of the perbenzylated β-cyclodextrin and fluorophore **4** (1 : 1 molar ratio), and is included to enable a direct determination of the benefits of covalent attachment in sensor design.

The synthesis of supramolecular hosts **S2** and **S3** is shown in Scheme 1. Perbenzylated β-cyclodextrin was obtained from the reaction of β-cyclodextrin with excess benzyl chloride.[17] Regioselective debenzylation of the primary rim was effected by treating the perbenzylated β-cyclodextrin with DIBAL-H.[18] This was followed by esterification[19] with the acid derivative of fluorophore **4**, yielding mono- and di-functionalized sensors **S2** and **S3**. Compounds **S2** and **S3** were fully characterized by ^{1}H NMR, ^{13}C NMR, MALDI-TOF mass spectrometry, and UV-visible and fluorescence spectroscopy.

The sensitivity of the fluorescence emission responses of sensors **S1–S3** to solvent composition were investigated, with the goal of ensuring full dissolution of the sensor while enabling strong binding of analytes in the cyclodextrin (optimal in aqueous environments). These competing considerations led us to choose an 80 : 20 water–DMSO mixture as the optimal sensing solvent. Of note, covalent attachment of the fluorophores in **S2** and **S3** led to a reduction of the fluorescence emission compared to the free fluorophore in **S1** (Fig. 4). This decrease is in agreement with literature precedent in analogous systems, and occurs as a result of increased non-radiative decay pathways that are available through covalent attachment to a highly flexible macromolecule. That decrease is offset by the markedly improved fluorescence modulation results in the presence of various analytes.[20]

The choice of perbenzylated β-cyclodextrin as a receptor is due to the strong binding of organic guest molecules in the extended hydrophobic cavity. A comparison of association constants of analyte **5** revealed a 1000-fold increase in the binding constant with perbenzylated β-cyclodextrin compared to β-cyclodextrin, with further increases in the fluorophore-functionalized cyclodextrins **S2** and **S3** (Table 1). These binding constants are orders of magnitude higher than the highest literature-reported binding constants for analyte **5** in β-cyclodextrin (K_a = 50–215 M^{-1}).[21] Higher association constants for analyte-sensor binding are known to lead to improved sensor performance,[22] a phenomenon that is also borne out in this system (*vide infra*).

Similarly, in this case, strong binding of analytes **5–8** in hosts **S1–S3** induced marked changes in the resulting fluorescence emission due to proximity-induced interactions between the analyte and the fluorophore. These changes were quantified according to eqn (1).

The sensor **S1** shows a fluorescence modulation value close to 1.00 for all the tested analytes, indicating minimal to no effect on the fluorescence emission of the fluorophore with the introduction of the analyte. In contrast to this, fluorescence modulation values measured for sensors **S2** and **S3** are significantly different from that of **S1**, and display widespread variability between

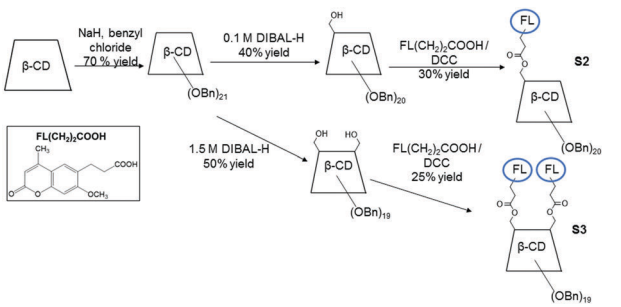

Scheme 1 Synthesis of supramolecular hosts **S2** and **S3**.

Table 1 Association constants of analyte **5** in perbenzylated β-cyclodextrin, **S2**, and **S3**[a]

Host	Association constant (M^{-1})
Perbenzylated β-cyclodextrin	3.6 (0.1) × 10^4
S2	4.8 (0.5) × 10^4
S3	24.9 (0.5) × 10^4

[a] Association constants calculated using ^{1}H NMR titrations in 80 : 20 water–DMSO mixture. Values in parentheses indicate the error in the association constant values.

Table 2 Fluorescence modulation of supramolecular sensors in the presence of aromatic alcohol analytes **5–8**[a]

Analyte	S1	S2	S3
5	1.00 ± 0.00	1.04 ± 0.01	0.98 ± 0.01
6	1.01 ± 0.00	0.82 ± 0.01	0.88 ± 0.01
7	0.99 ± 0.00	0.90 ± 0.00	1.05 ± 0.02
8	1.01 ± 0.01	0.87 ± 0.01	0.75 ± 0.01

[a] Results were calculated using eqn (1). All results represent an average of at least 3 trials.

different classes of analytes as well as within each analyte class (Table 2). These results clearly demonstrate the effect of the sensor architecture, and in particular the effects of covalent fluorophore attachment and the number of fluorophore units. The covalent attachment ensures close proximity between the cyclodextrin-bound analyte and the fluorophore moiety(ies), causing various degrees of fluorescence modulation to occur. An example of analyte-induced fluorescence modulation for analyte **8** is shown in Fig. 5.

The fluorescence signals of sensors **S1–S3** in the presence of analytes **5–8** were subjected to linear discriminant analysis, and enabled 100% selectivity between the different aromatic alcohol isomers (Fig. 6). This selectivity is particularly noteworthy as such isomers are challenging to separate using other analytical techniques.[23] The binding of other structural isomers and analogues in supramolecular hosts **S1–S3** also led to analyte-specific changes in the fluorescence emission (Table 3), with selected results highlighted in Fig. 7–10.

Analytes **9–12** represent a class of aliphatic alcohols consisting of cyclohexylmethanol (**11**) and its isomers. These compounds are widely used as alkene precursors,[24] and a structurally similar analogue was part of a recent chemical spill.[25] While all the analytes are structural isomers, analytes **10** and **12** are also stereoisomers. Distinct fluorescence modulation values are noted for sensor **S3** in combination with stereoisomers **10** and **12**, highlighting the power of the cyclodextrin-based sensor in differentiating even small structural changes. Overall, the use of sensors **S1–S3** in combination with these analytes enabled 100% differentiation using linear discriminant analysis (Fig. 7).

Analytes **13–16** represents aromatic pesticide *p*,*p*-DDT (compound **15**), its known metabolites DDE (compound **13**) and DDD (compound **14**),[26] and its co-occurring structural isomer *o*,*p*-DDT (compound **16**).[27] These compounds are suspected carcinogens[28] and toxicants,[29] and are important targets for detection. Despite the structural similarity between the analytes,

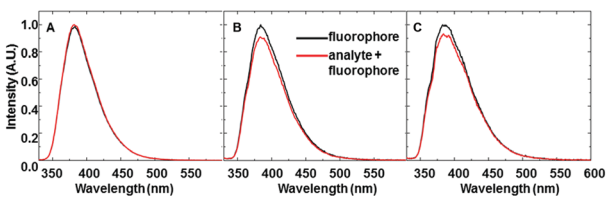

Fig. 5 Fluorescence emission of (A) sensor **S1**; (B) sensor **S2**; and (C) sensor **S3** in the presence of analyte **8**. (λ_{ex} = 320 nm; 3 nm excitation slit width; 3 nm emission slit width).

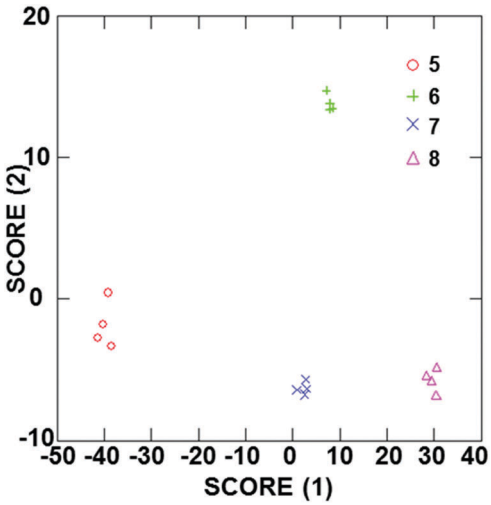

Fig. 6 Linear discriminant analysis showing 100% differentiation between analytes **5–8** based on their interactions with supramolecular hosts **S1–S3**.

Table 3 Fluorescence modulation of sensors **S1–S3** in the presence of analytes **9–26**[a]

Analyte	S1	S2	S3
9	1.01 ± 0.00	0.89 ± 0.00	1.07 ± 0.05
10	1.01 ± 0.00	0.90 ± 0.00	0.97 ± 0.01
11	1.01 ± 0.00	0.99 ± 0.03	0.77 ± 0.06
12	0.99 ± 0.00	0.89 ± 0.00	1.14 ± 0.01
13	1.00 ± 0.00	0.93 ± 0.01	1.33 ± 0.03
14	1.01 ± 0.00	0.95 ± 0.01	1.07 ± 0.04
15	0.98 ± 0.01	1.17 ± 0.01	1.35 ± 0.05
16	0.99 ± 0.01	1.08 ± 0.01	1.04 ± 0.05
17	1.00 ± 0.00	1.01 ± 0.01	0.94 ± 0.02
18	1.05 ± 0.00	1.06 ± 0.00	0.93 ± 0.02
19	0.98 ± 0.00	1.09 ± 0.01	0.95 ± 0.02
20	1.00 ± 0.00	0.99 ± 0.01	1.01 ± 0.01
21	1.03 ± 0.01	1.03 ± 0.02	0.89 ± 0.01
22	1.03 ± 0.00	1.06 ± 0.06	0.85 ± 0.01
23	1.01 ± 0.01	1.02 ± 0.04	0.98 ± 0.03
24	1.01 ± 0.00	1.07 ± 0.04	0.89 ± 0.02
25	1.05 ± 0.00	0.56 ± 0.01	0.98 ± 0.01
26	1.00 ± 0.01	0.92 ± 0.03	1.14 ± 0.02

[a] Fluorescence modulation results were calculated using eqn (1). All results represent an average of at least 3 trials.

100% accurate classification was achieved (Fig. 8). Interestingly, although sensor **S3** demonstrated nearly identical fluorescence modulation values in response to analytes **13** and **15**, sensor **S2** was able to clearly differentiate between those two analytes. These results illustrate that altering the degree of functionalization of the sensor can alter its response.

Analytes **17–21** represent aliphatic *n*-hexane (compound **17**), its commonly occurring structural isomers (compounds **18–20**, generated in 10–30% yield from industrial production of hexane)[30] and its cyclopentane analogue (compound **21**). The fact that hexanes co-occur as isomeric mixtures complicates a variety of applications that require accurate characterization.[31] Using this supramolecular sensing strategy, 100% accurate classification between these analytes is achieved (Fig. 9).

Analytes **22–26** represent polychlorinated biphenyls (PCBs), a class of POPs that cause neurotoxicity[32] and endocrine disruption.[33]

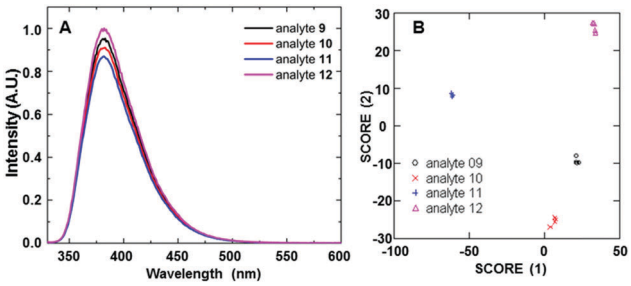

Fig. 7 (A) Fluorescence response of host **S1** in the presence of analytes **9–12**; (B) linear discriminant analysis of the fluorescence responses, leading to 100% differentiation of the analyte signals (λ_{ex} = 320 nm; 3 nm excitation slit width; 3 nm emission slit width).

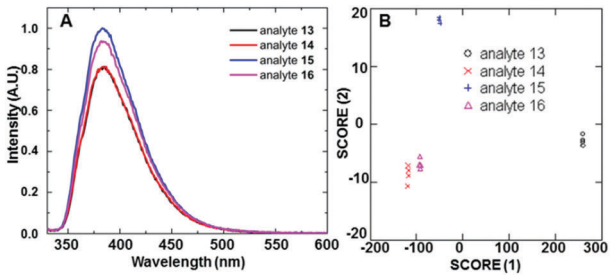

Fig. 8 (A) Fluorescence response of host **S2** in the presence of analytes **13–16**; (B) linear discriminant analysis of the fluorescence responses, leading to 100% differentiation of the analyte signals (λ_{ex} = 320 nm; 3 nm excitation slit width; 3 nm emission slit width).

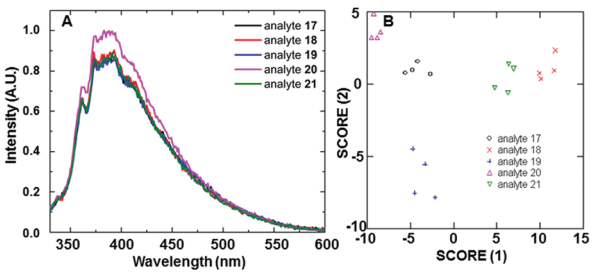

Fig. 9 (A) Fluorescence response of host **S3** in the presence of analytes **17–21**; (B) linear discriminant analysis of the fluorescence responses, leading to 100% differentiation of the analyte signals (λ_{ex} = 320 nm; 3 nm excitation slit width; 3 nm emission slit width).

As a result of these effects, the use of PCBs has been banned in many countries; however, their environmental persistence means that significant amounts of PCBs are still found in the environment.[34] 100% accurate classification has been achieved for these analytes (Fig. 10), which is particularly crucial because these analytes have widely disparate toxicities.

The ability of this detection method to generate well-separated signals was further investigated by generating an array with all analytes from all classes. In this case, the array exhibited well-separated clusters based on compound class, as well as excellent separation within each class. Overall, 100% accurate identification was obtained (see ESI† for more details).

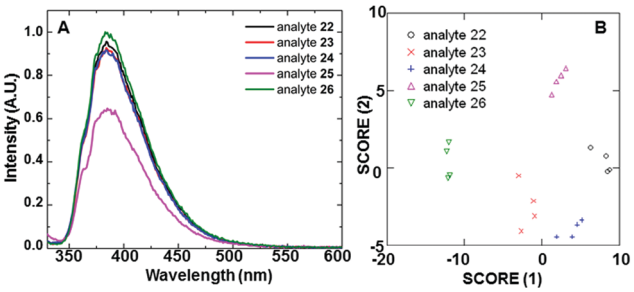

Fig. 10 (A) Fluorescence response of host **S2** in the presence of analytes **22–26**; (B) linear discriminant analysis of the fluorescence responses, leading to 100% differentiation of the analyte signals (λ_{ex} = 320 nm; 3 nm excitation slit width; 3 nm emission slit width).

Table 4 Calculated limits of detection and comparisons to known levels of concern

Analytes	Sensors	LOD calculated (μM)	Limit of concern (μM)
5	**S2**	7.1 ± 0.9	[a]
6	**S1**	5.5 ± 0.2	21.27[35]
6	**S3**	7.3 ± 0.5	21.27[35]
11	**S1**	1.2 ± 0.01	[a]
11	**S2**	1.4 ± 0.1	[a]
15	**S1**	0.43 ± 0.04	2.82[36]
15	**S2**	0.48 ± 0.05	2.82[36]
15	**S3**	2.1 ± 0.03	2.82[36]
18	**S1**	2.1 ± 0.2	5801.81[37]
19	**S2**	21.1 ± 1.4	5801.81[38]
21	**S3**	8.4 ± 0.6	[a]
22	**S3**	5.2 ± 0.2	1.00[38]
25	**S1**	0.30 ± 0.01	1.71[39]
26	**S2**	0.17 ± 0.01	1.00[38]

[a] Limits of concern have not been established for these compounds.

The limits of detection for each sensor **S1**, **S2** and **S3** for each class of analytes were calculated, to determine their ability to sense analytes at environmental levels of concern and at levels that induce toxicity. In every case, the calculated limits of detection were at or below the literature reported limits of concern (Table 4), highlighting the sensitivity of this method.

Practical applications of this system require the capability to identify analyte mixtures, because environmental contamination scenarios almost always involve such mixtures. To that end, preliminary work focused on identification of 1 : 1 binary mixtures of aromatic alcohol analytes **5–8**. Using the supramolecular sensors combined with linear discriminant analytical techniques, 83% accurate identification of the 1 : 1 binary mixtures was obtained (Fig. 11). Interestingly, the mixture of analytes **5** + **7** is grouped near the mixtures of analytes **6** + **8** and **5** + **8**, which reduces the overall classification accuracy slightly. This kind of co-clustering of analyte groups has been observed previously, and can be attributed to similar sensor responses originating from competing interactions between each component of the mixture. Other than those combinations, the mixtures demonstrated excellent signal separation and accurate identification. Current work in our group is focused on improving classification accuracy of analyte mixtures, expanding such techniques to multiple analyte classes, and moving from binary mixtures to ternary and even quaternary mixtures of analytes.

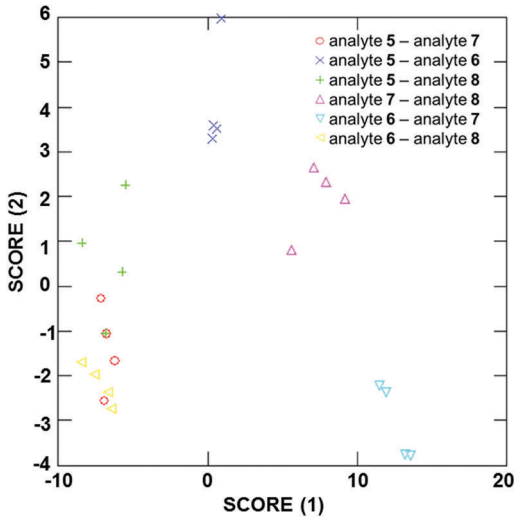

Fig. 11 Linear discriminant analysis results of binary mixtures of analytes **5–8**.

Conclusions

In conclusion, we have developed an efficient array-based detection strategy for isomeric and analogous analytes. The array employs three architecturally unique perbenzylated β-cyclodextrin–fluorophore sensors for identification of a particular isomer within a class of isomeric or structurally similar analytes. The binding of analytes to the cyclodextrin induces a distinct change in the fluorescence emission of the attached fluorophores, which is then statistically translated into array clusters of maximum separation *via* linear discriminant analysis. We demonstrate 100% successful classification of three isomeric (aromatic alcohols, aliphatic alcohols, aliphatic hexanes) and two analogous (DDT pesticides, PCB congeners) analyte classes. Sensitivity measurements highlight limits of detection at or near literature-reported levels of concern. Preliminary attempts on binary mixtures demonstrated fairly selective levels of classification with 83% accuracy. This method in tandem with chromatographic analysis of complex isomeric mixtures would complement each other in determining the nature of each isomer. Current work in our laboratory is focused on expanding the classes of analytes detectable *via* this system, improving analyte mixture identification, and developing a practical cyclodextrin-based detection device. The results of these and other investigations will be reported in due course.

Conflicts of interest

There are no conflicts of interest to declare.

Acknowledgements

This work was supported by the National Science Foundation (Grant Number 1453483) and the National Cancer Institute (Grant Number CA185435).

References

1 K. L. Willett, E. M. Ulrich and R. A. Hites, *Environ. Sci. Technol.*, 1998, **32**, 2197.
2 I. Rodriguez, M. Fraga, A. Alfonso, D. Guillebault, L. Medlin, J. Baudart, P. Jacob, K. Helmi, T. Meyer, U. Breitenbach, N. M. Holden, B. Boots, R. Spurio, L. Cimarelli, L. Mancini, S. Marcheggiani, M. Albay, R. Akcaalan, L. Koeker and L. M. Botana, *Environ. Toxicol. Chem.*, 2017, **36**, 645.
3 M. Bergknut, A. Kucera, K. Frech, E. Andersson, M. Engwall, U. Rannug, V. Koci, P. L. Andersson, P. Haglund and M. Tysklind, *Environ. Toxicol. Chem.*, 2007, **26**, 208.
4 U. Shafique, S. Schulze, C. Slawik, S. Kunz, A. Paschke and G. Schueuermann, *Anal. Chim. Acta*, 2017, **949**, 8.
5 J. E. Rager, M. J. Strynar, S. Liang, R. L. McMahen, A. M. Richard, C. M. Grulke, J. F. Wambaugh, K. K. Isaacs, R. Judson, A. J. Williams and J. R. Sobus, *Environ. Int.*, 2016, **88**, 269.
6 O. R. Miranda, B. Creran and V. M. Rotello, *Curr. Opin. Chem. Biol.*, 2010, **14**, 728; K. L. Diehl and E. V. Anslyn, *Chem. Soc. Rev.*, 2013, **42**, 8596.
7 X. Xu, Z. Liu, X. Zhang, S. Duan, S. Xu and C. Zhou, *Electrochim. Acta*, 2011, **58**, 142; X. Chen, X. Cheng and J. J. Gooding, *Anal. Chem.*, 2012, **84**, 8557.
8 S. Hussain, A. H. Malik and P. K. Iyer, *J. Mater. Chem. B*, 2016, **4**, 4439.
9 B. B. Prasad and I. Pandey, *Sens. Actuators, B*, 2013, **181**, 596.
10 J. Zhang, X. Zhang, J. Chen, C. Deng, N. Xu, W. Shi and P. Cheng, *Inorg. Chem. Commun.*, 2016, **69**, 1.
11 S. Hatanaka, T. Ono and Y. Hisaeda, *Chem. – Eur. J.*, 2016, **22**, 10346; S. Mukherjee, A. V. Desai, A. I. Inamdar, B. Manna and S. K. Ghosh, *Cryst. Growth Des.*, 2015, **15**, 3493; B. Gole, W. Song, M. Lackinger and P. S. Mukherjee, *Chem. – Eur. J.*, 2014, **20**, 13662.
12 E. A. Cohen Hubal, A. Richard, L. Aylward, S. Edwards, J. Gallagher, M.-R. Goldsmith, S. Isukapalli, R. Tornero-Velez, E. Weber and R. J. Kavlock, *J. Toxicol. Environ. Health*, 2010, **13**, 299.
13 L. J. Gensburg, C. Pantea, C. Kielb, E. Fitzgerald, A. Stark and N. Kim, *Environ. Health Perspect.*, 2009, **117**, 1265.
14 D. Megson, E. J. Reiner, K. J. Jobst, F. L. Dorman, M. Robson and J.-F. Focant, *Anal. Chim. Acta*, 2016, **941**, 10.
15 D. J. DiScenza and M. Levine, *New J. Chem.*, 2016, **40**, 789; N. Serio, D. F. Moyano, V. M. Rotello and M. Levine, *Chem. Commun.*, 2015, **51**, 11615; N. Serio, K. Miller and M. Levine, *Chem. Commun.*, 2013, **49**, 4821.
16 K. Higashi, S. Ideura, H. Waraya, W. Limwikrant, K. Moribe and K. Yamamoto, *Chem. Pharm. Bull.*, 2010, **58**, 769.
17 J. Bjerre, T. H. Fenger, L. G. Marinescu and M. Bols, *Eur. J. Org. Chem.*, 2007, 704.
18 T. Lecourt, A. Herault, A. J. Pearce, M. Sollogoub and P. Sinay, *Chem. – Eur. J.*, 2004, **10**, 2960.
19 B. S. Choi, J. Choi, S. Bak and S. Koo, *Eur. J. Org. Chem.*, 2015, 514.
20 C. Huo, J.-C. Chambron and M. Meyer, *New J. Chem.*, 2008, **32**, 1536.

21 G. W. Meindersma, T. van Schoonhoven, B. Kuzmanovic and A. B. de Haan, *Chem. Eng. Process.*, 2006, **45**, 175.
22 R. N. Dsouza, U. Pischel and W. M. Nau, *Chem. Rev.*, 2011, **111**, 7941.
23 J. Peng, Y. Zhang, X. Yang and M. Qi, *J. Chromatogr. A*, 2016, **1466**, 148.
24 J. J. Cawley and P. E. Lindner, *J. Chem. Educ.*, 1997, **74**, 102.
25 A. J. Whelton, L. McMillan, M. Connell, K. M. Kelley, J. P. Gill, K. D. White, R. Gupta, R. Dey and C. Novy, *Environ. Sci. Technol.*, 2015, **49**, 813.
26 M. Ricking and J. Schwarzbauer, *Environ. Chem. Lett.*, 2012, **10**, 317.
27 J. P. Arrebola, M. Cuellar, J. P. Bonde, B. Gonzalez-Alzaga and L. A. Mercado, *Environ. Res.*, 2016, **151**, 469.
28 A. M. Soto, K. L. Chung and C. Sonnenschein, *Environ. Health Perspect.*, 1994, **102**, 380.
29 A. Mansouri, M. Cregut, C. Abbes, M.-J. Durand, A. Landoulsi and G. Thouand, *Appl. Biochem. Biotechnol.*, 2017, **181**, 309.
30 R. A. Myers, *Handbook of Petroleum Refining Process*, McGraw-Hill, New York, 2004; R. Clavier, *Wiley Critical Content: Petroleum Technology*, Wiley-Interscience, Hoboken, New Jersey, 2007.
31 R. Hayati, S. Z. Abghari, S. Sadighi and M. Bayat, *Korean J. Chem. Eng.*, 2015, **32**, 629.
32 G. Winneke, *J. Neurol. Sci.*, 2011, **308**, 9.
33 T. Grzeskowiak, B. Czarczynska-Goslinska and A. Zgola-Grzeskowiak, *TrAC, Trends Anal. Chem.*, 2016, **75**, 209.
34 N. S. Shifrin and A. P. Toole, *Environ. Eng. Sci.*, 1998, **15**, 247.
35 Center for Disease Control and Prevention. The National Institute for Occupational Safety and Health (NIOSH): Cresols (o, m, p isomers) https://www.cdc.gov/niosh/idlh/cresol.html, accessed Dec 20, 2016.
36 Center for Disease Control and Prevention. The National Institute for Occupational Safety and Health (NIOSH): DDT https://www.cdc.gov/niosh/idlh/50293.html, accessed Dec 20, 2016.
37 Center for Disease Control and Prevention. The National Institute for Occupational Safety and Health (NIOSH): 2-methylpentane. https://www.cdc.gov/niosh/ipcsneng/neng1262.html, accessed Dec 20, 2016.
38 Center for Disease Control and Prevention. The National Institute for Occupational Safety and Health (NIOSH): 3-methylpentane. https://www.cdc.gov/niosh/ipcsneng/neng1263.html, accessed Dec 20, 2016.
39 Center for Disease Control and Prevention. The National Institute for Occupational Safety and Health (NIOSH): Polychlorinated Biphenyls (PCB's). https://www.cdc.gov/niosh/docs/86-111/default.html, accessed Dec 20, 2016.